scientific reports

Check for updates

OPEN

Preparation of plane trees' bark biochar/ZnAl-LDH and its adsorption performance for phosphate and recovery

Lihui Zhang[1,2]✉, Chen Zhang[1,2], Caoyang Zhang[1], Weili Li[1], Yanbiao Zhou[1], Yabo Wang[1] & Gangfeng Du[1]

Biochar is an excellent adsorbent for organic pollutants, but the removal effect for inorganic phosphorus is not satisfactory. In order to improve its phosphorus removal effect, ZnAl-LDH modified plane trees' bark biochar was presented in this paper. The plane trees' bark biochar was prepared by chemical-activation method by utilizing K_2CO_3 as the activation agent. And then, ZnAl-LDH modified biochar was prepared by in-situ co-precipitation method with ammonia as the precipitate agent. As the sample was as little as 10 mg, the adsorption ratio was about 93% for the 25 mL of 20 mg/L PO_4^{3-}. The saturated adsorption capacity for PO_4^{3-} was 103.1 mg/g, calculated by Langmuir equation, revealing the adsorption was mainly mono-molecular layer adsorption. The possible adsorption mechanism of phosphate mainly contained interlayer anion exchange, surface complexion and ligand exchange. Moreover, the absorbed sample were soaked in 5.5% Na_2CO_3 solution for phosphate desorption, nearly 60% of the absorbed phosphate could be recovered and may reuse in the future.

Keywords Plane trees' bark biochar, Zn-Al hydrotalcite, Phosphate, Adsorption property, Phosphorus recover

Phosphorus is widely used in the field of industries and agriculture. If phosphorus containing wastewater is discharged to the surface water, it will lead to eutrophication of rivers, lakes, and other water bodies. That not only pollutes the environment, but also poses the threat to human health. Therefore, it is emergency for phosphorus removal to control water eutrophication for the environment. At present, the following methods are used for phosphorus removal, such as chemical precipitation[1], ion exchange[2], and adsorption[3]. Among them, adsorption method is relatively simple, low-costs, and relatively green to the environment, so adsorption process is more practical in wastewater treatment. In the literature, the materials for phosphorus removal by adsorption method include Mn-based metal-organic framework[4], 3D rice-like lanthanum-doped nanocomposites[5], hydrotalcite-like materials[6], metal hydroxides (such as nickel hydroxide[7], and so on. Hydrotalcites (LDHs) can be represented by the following general formula, where M^{2+} is divalent ions such as Mg^{2+}, Ni^{2+}, Co^{2+}, and M^{3+} is trivalent ions such as Al^{3+}, Fe^{3+}, Cr^{3+}. X is the molar ratio of $M^{3+}/(M^{2+} + M^{3+})$. A_n^- is the interlayer anion (Cl^-, OH^-, etc.) to balance the charge. LDHs show good anion exchange ability such as phosphate ions due to their interlayer anion mobility and surface complexation[8–12].

Biomass-based activated carbon were produced by utilizing agricultural and forestry waste as the sources. The biomass has many advantages such as wide sources, low price, reproducible, and green environmental protection, making it a good choice as the source of active carbon. The obtained biochar has a porous surface structure, rich functional groups and show excellent adsorption capacity for organic pollutant. Plane Tree is widely planted in the world, which is able to adsorb harmful gases. The voucher specimen of plane tree is deposited in a publicly herbarium such as French National Museum of Natural History Herbarium. In this paper, the plane trees' bark naturally shed in Pingdingshan University was used as the raw material to prepare K_2CO_3-activated biochar. However, due to the negative surface charge of the biochar, its adsorption performance for phosphate ions is limited. LDHs loaded onto biochar in a composite is therefore a successful strategy for improving the adsorption properties. Co- precipitation is the preferred way for large-scale production of LDH/BC, due to their low-cost and low energy consumption, and high-yield advantages[9,13]. Moreover, LDHs on the biochar can reduce its agglomeration, and increase its specific surface area, which could contribute to high

[1]School of Chemistry and Environment Engineering, Pingdingshan University, 467000 Pingdingshan, China. [2]These authors jointly supervised this work: Lihui Zhang and Chen Zhang. ✉email: 15290759930@139.com

adsorption capacity. At the same time, the leaching of LDH could diminish in aqueous solution, which is safer for water environment. It is more practical that the absorbed phosphate in the hydrotalcite-like materials could be recovered in the Na_2CO_3 solution, making it possible for phosphorus recycling and re-utilization[14]. Herein, the biochar/ZnAl-LDH composites were synthesized for phosphate removal, and phosphorus removal efficiency was evaluated. The isothermal adsorption and adsorption kinetics of the adsorption process were investigated. Moreover, the possible adsorption mechanism was analyzed in the last part of the manuscript.

Materials and methods

Preparation of plane trees' bark biochar/ZnAl-LDH composite

Plane trees' bark was used as raw materials for biochar, which was collected in Pingdingshan University in Summer. The plane trees' bark was crushed and passed through 100 mesh to obtain the fine powder. 5 g of the plane trees' powder was mixed with 12 mL of 2 mol/L potassium carbonate solution drop by drop by stirring. After thorough mixing, the sample was sealed and soaked with potassium carbonate solution for 24 h at the room temperature. Then, the biochar was obtained by pyrolysis at 800 ℃ for 2 h. The resulting biochar was mixed with 20 mL of 1 mol/L HCl to remove the impurity, washed with distilled water until pH value was neutral, and dried at 110 ℃ for 2 h. The solid sample was further ground into powder to obtain plane trees' biochar. The ZnAl-LDH modified plane trees' biochar was prepared by in-situ co-precipitation process. The process was as follows: firstly, 1.73 g $ZnSO_4{\cdot}7H_2O$ and 1.33 g $Al_2(SO_4)_3{\cdot}18H_2O$ (the molar ratio of Zn^{2+}:Al^{3+} 3:1) were dissolved in the 20 mL of distilled water. Then, the solution was added to 0.5 g of biochar by string, followed by stirring treatment for another 20 min. After that, the pH of the above solution was adjusted to 10 by ammonia solution. After aging treatment at 80 °C for 12 h, the sample was filtered, washed by distilled water for 3 times until pH was neutral, and collected after drying at 80 °C for 12 h to obtain ZnAl-LDH modified plane trees' biochar. For comparison, Zn_3Al-LDH was prepared using the same method.

Characterization of absorbent

Crystal structure of these samples were identified by a X-ray diffractometer (XRD) via a D8-ADVANCE instrument with the scanning range from 10° to 80° in the 2θ range. The morphology and composition were inspected using a field emission scanning electron microscope (SEM-EDX; Gemini 500). The functional groups of synthesized adsorbents were analyzed by a Fourier transform infrared spectroscopy (FTIR, Nicolet 5700) and X-ray photoelectron spectroscopy (XPS, Thermo Scientific K-Alpha, USA).

Batch adsorption experiments

Batch adsorption experiments of phosphate by biochar/ZnAl-LDH were carried out by using10 mg of sample, 25 mL of phosphate solution at a speed of 120 rpm in a rotational shaker. The effects of initial concentration (20、40、60、80、100、125、150 mg/L), adsorption time (5、10、15、30、45、60、120 min) and temperature (25℃、35℃、45℃) on adsorption effect were investigated. After adsorption process, the adsorption solution was filtered, and the remaining content of phosphate in the solution was measured by phosphomolybdate blue spectrophotometry. The removal efficiency (*R*), adsorption capacity (Q_e) were calculated.

$$R\,(\%) = \frac{C_0 - C_e}{C_0} \times\ 100\%$$

$$Q_e = \frac{\mathrm{v}(C_0 - C_e)}{\mathrm{m}}$$

Where C_0 and C_e represent the initial concentration and equilibrium concentration of PO_4^{3-} in solution (mg/L), respectively. V is the volume of solution (L), and m is the mass of absorbent (g).

The adsorption kinetics and isothermal adsorption were analyzed based on the data by the following model. The isothermal adsorption process could be analyzed by The classic Langmuir (1) and Freundlich isotherm models (2):

$$\frac{1}{Q_e} = \frac{1}{Q_{max}k_L C_e} + \frac{1}{Q_{max}} \tag{1}$$

$$lnQ_e = lnk_F + \frac{1}{n}lnC_e \tag{2}$$

Where Q_e and Q_{max}(mg/g) represent the equilibrium and highest adsorption capacity, respectively. C_e is the equilibrium concentration of PO_4^{3-}. In the Langmuir isotherms (1), $\frac{1}{Q_e}$- $\frac{1}{C_e}$ shows linear relationships, the Q_{max} and k_L constants can be determined from the slope and the intercept of the line. Moreover, in the Freundlich isotherms (2), lnQ_e- lnC_e shows linear relationships, the Freundlich constants k_F and n can be determined from the slope and the intercept of the line.

The pseudo-first order kinetic mode (1) and pseudo-second order kinetic mode (2) are described as follows:

$$ln(Q_e - Q_t) = lnQ_{e,cal} - \frac{k_1 t}{2.303} \tag{3}$$

$$\frac{t}{Q_t} = \frac{t}{Q_{e,cal}} + \frac{1}{k_2 Q_{e,cal}^2} \tag{4}$$

Where Q_t and Q_e (mg/g) are the amount of PO_4^{3-} absorbed at time t and equilibrium time, respectively. In the pseudo-first order kinetic model, when $\ln(Q_e - Q_t)$ is plotted versus t, the $Q_{e,cal}$ and k_1 constants can be determined from the slope and the intercept of the line. In the pseudo-second order kinetic model, When t/Q_t is plotted versus t, the $Q_{e,cal}$ and k_2 constants can be determined from the slope and the intercept of the line.

Results and discussion

Absorbent physicochemical characteristics

Figure 1 showed the XRD patterns of the plane trees' bark biochar, ZnAl-LDH, ZnAl -LDH modified plane trees' bark biochar and ZnAl-LDH modified plane trees' bark biochar after phosphate adsorption. As shown in Fig. 1a, it could be revealed that there are two typical characteristic peaks of activated carbon at $2\theta = 24.5^o$ and 43^o, without any impurities. Figure 1b showed the XRD patterns of Zn_3Al-LDH. The samples showed the obvious diffraction peaks at $2\theta = 10.2^o$, 20.3^o, 34.7^o, 62.1^o, which conformed to (003), (006), (009) and (110) crystal faces of hydrotalcites. Compared to activated carbon, the ZnAl-LDH/biochar in Fig. 1c exhibited characteristic peaks at $2\theta = 11.21^o$, 21.87^o, 35.20^o, 62.10^o, corresponding to (003), (006), (009) and (110) crystal plane, respectively[9,13]. The above results showed that the Zn-Al LDH was successfully modified onto plane trees' biochar. The diffraction peak shape was relatively sharp, good symmetry, indicating the formed ZnAl-LDH onto the biochar possessed good crystal structure and high crystallinity. After phosphate adsorption, the position of the diffraction peaks remained unchanged in Fig. 1d, indicating that the adsorbed phosphate was mainly intercalated in the layers of the hydrotalcite.

As shown in Fig. 2, in the FTIR spectrum of biochar, the broad band at 3422 cm^{-1} originated from stretching vibration of O-H. The peaks at 1566 cm^{-1} and 1470 cm^{-1} attributed to the stretching vibration peaks of C = O and C = C, respectively. In the FTIR spectrum of ZnAl-LDH, the broad band at 3400 cm^{-1} attributed to the stretching vibration of laminated (M)-OH, 1600 cm^{-1} was the bending vibration of interlayer H-O-H, and 1100 cm^{-1} was absorption peak of interlayer sulfate ions. Moreover, the peaks at 427 cm^{-1} and 612 cm^{-1} belonged to lattice vibrations of Al-O and Mg-O, respectively[14,15]. In the BC/ZnAl-LDH composites, the characteristic absorption peaks of hydrotalcite was observed. Therefore, hydrotalcite loaded onto biochar hold promise for effective absorption of phosphate.

As shown in Fig. 3a and b, the biochar showed honeycomb-shaped pores with smaller sizes. Moreover, the as-prepared ZnAl-LDH was shown in the layered stacking structure in Fig. 3c. The biochar/ZnAl-LDH exhibited both the porous structure and layered structure in Fig. 3d, indicating the formed composites. Combined with the XRD results, the ZnAl-LDH was successfully in-situ precipitated onto the biochar. The ZnAl-LDH modified biochar might have good phosphorus removal capacity, owing to the component of the hydrotalcites.

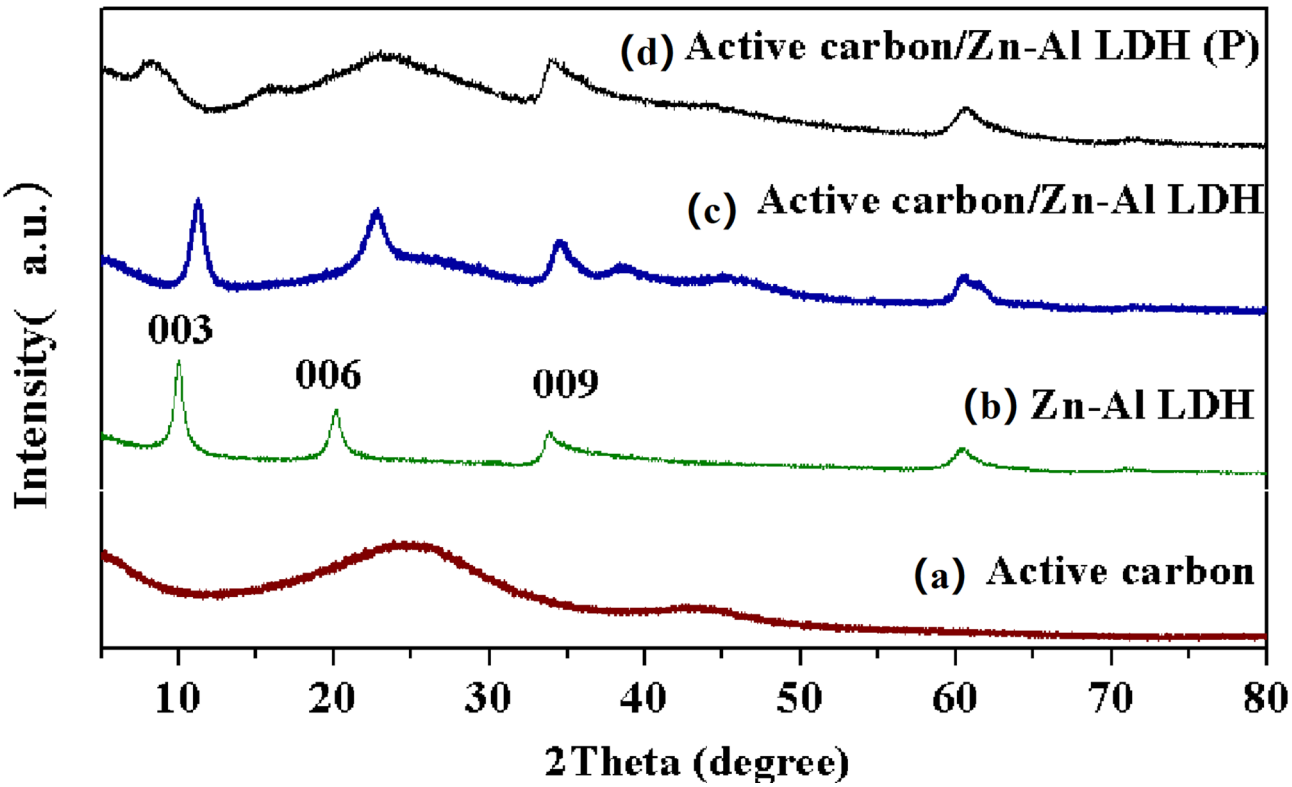

Fig. 1. Powder X-ray patterns of samples: (**a**) plane trees' bark biochar; (**b**) ZnAl-LDH; (**c**) ZnAl -LDH modified plane trees' bark biochar; (**d**) ZnAl-LDH modified plane trees' bark biochar after phosphate adsorption.

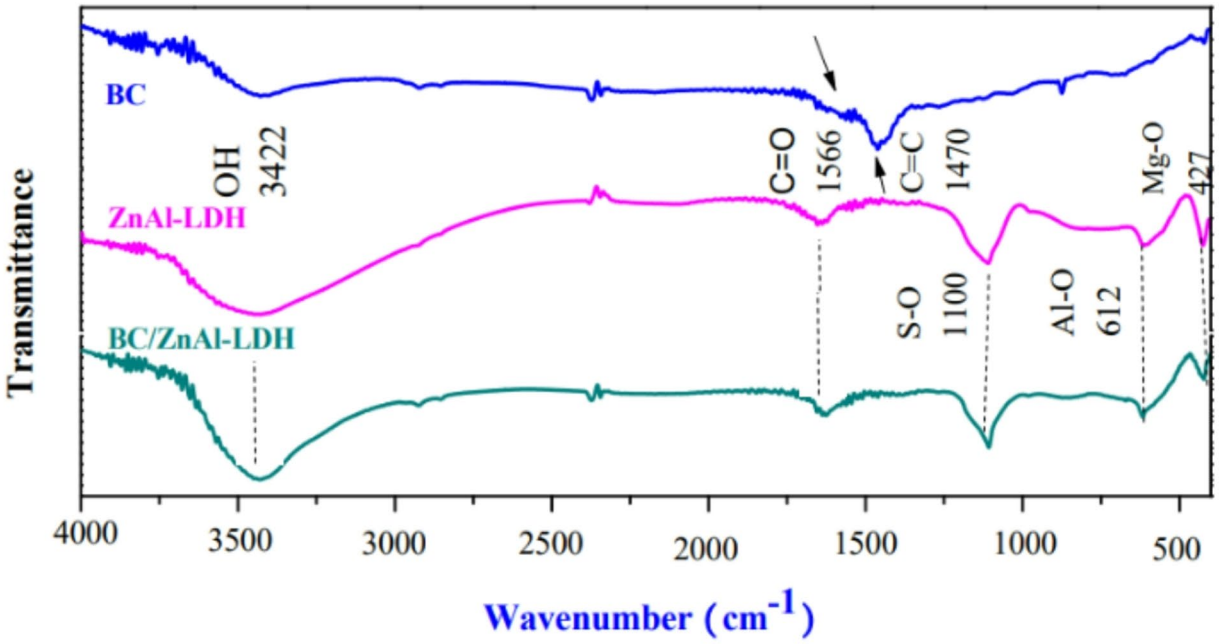

Fig. 2. FT-IR spectra of plane trees'bark biochar, ZnAl-LDH, and biochar/ZnAl-LDH.

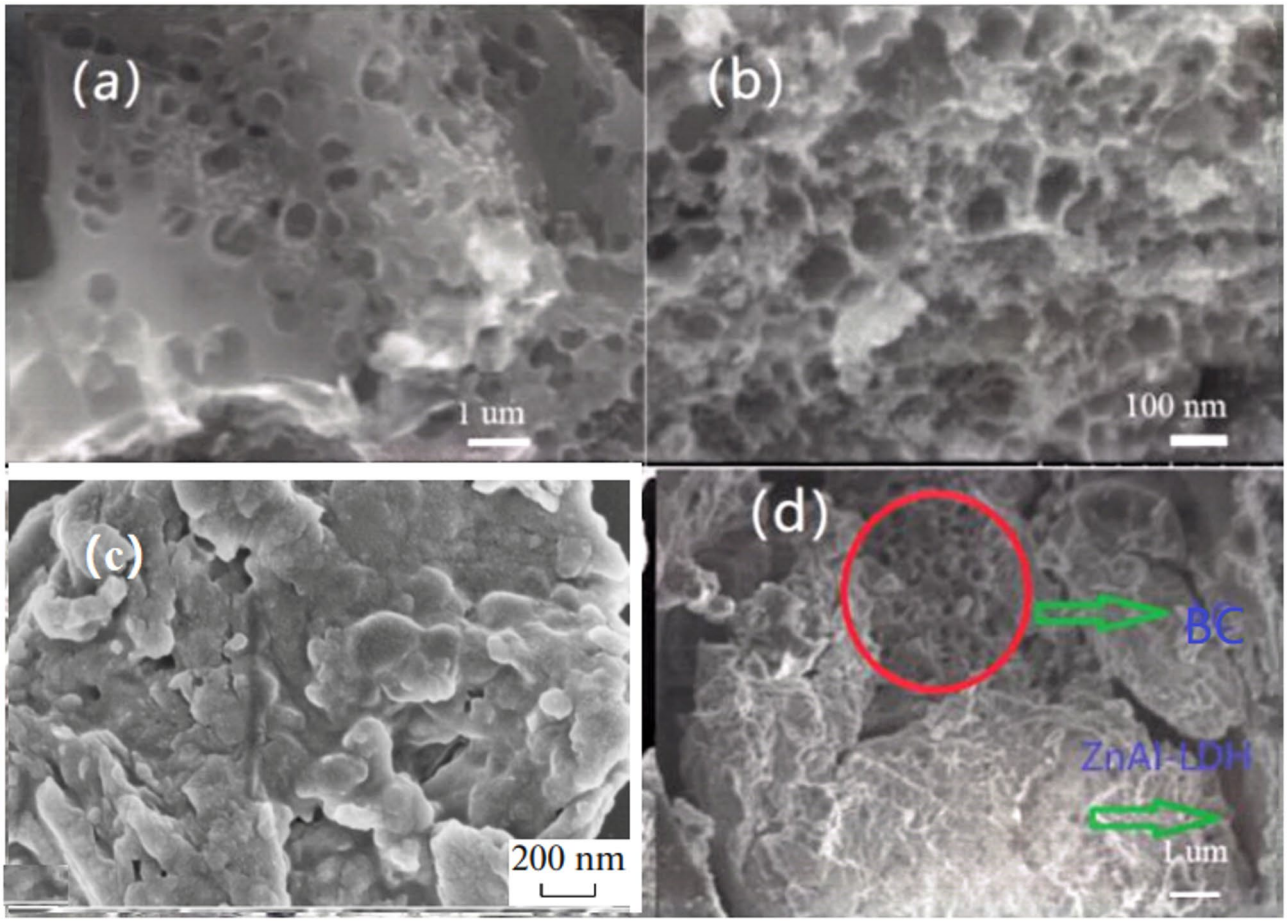

Fig. 3. SEM images of materials: (**a**, **b**) biochar; (**c**) ZnAl-LDH; (**d**) biochar/ZnAl-LDH.

Influence factors for adsorption

According to the experimental research, the adsorption effect of plane trees' bark biochar/ZnAl-LDH for phosphate on different initial concentrations was shown in Fig. 4a. Plane trees' bark biochar/ZnAl-LDH composites had a good adsorption effect for phosphate. As the sample was as little as 10 mg, the adsorption ratio was about 93% for the 25 mL of 20 mg/L PO_4^{3-}. Moreover, as the initial concentration of phosphate ions increased, the overall adsorption ratio of the sample decreases. This was mainly because the sample dosage was only 10 mg, the number of adsorption sites provided was limited. As the initial concentration of phosphate increased, adsorption sites was occupied by phosphate molecular until the active site was completely occupied. The remaining phosphate ions were free in the solution, and the adsorption ratio was low. As shown in Fig. 4b, the single biochar showed little adsorption effect for phosphate, compared to the blue adsorption mother liquor in the first volumetric flask. The third solution in the volumetric flask was colorless after adsorption (10 mg of biochar/ZnAl-LDH, 25 mL, 20 mg/L). The experimental results indicated that the phosphorus removal was successfully achieved by loading Zinc Aluminum hydrotalcite onto activated carbon, which expanded the application of activated carbon in water treatment.

According to the experimental research, the adsorption effects of plane trees' bark biochar/ZnAl-LDH at 20 mg/L phosphate at different adsorption time was shown in Fig. 4c. The adsorption ratio had reached 60% in the first 5 min, indicating that the adsorption process was very efficient. As the adsorption time increased, the adsorption ratio of phosphate ions continuously increased. And then, the adsorption process gradually became very slow, and finally reached equilibrium in the two hours. At the initial stage, the plane trees' bark biochar/ZnAl-LDH composites could provide more adsorption sites. The concentration of phosphate in the aqueous solution was relatively high, and the adsorption driving force between the material and the adsorbate P was so large that the adsorption rate at the initial stage was very fast. Therefore, the adsorption ratio was as high as 72% in the first 5 min. As the adsorption time increased, the adsorption reached an equilibrium state. Therefore,

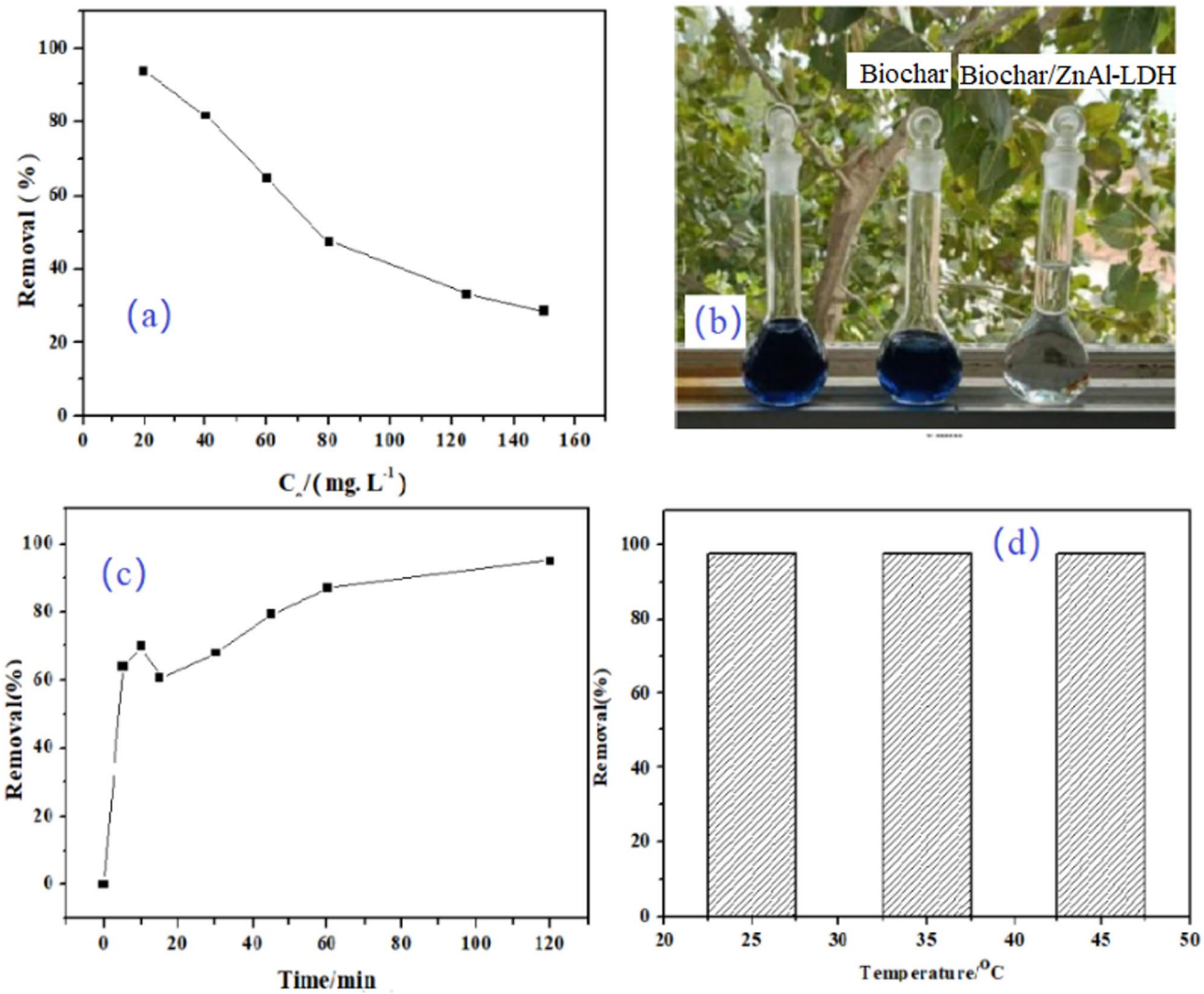

Fig. 4. Effects of initial concentration (**a**), adsorption effect (**b**), and adsorption time (**c**), temperature (**d**) on phosphorus removal by plane trees' bark/ZnAl-LDH.

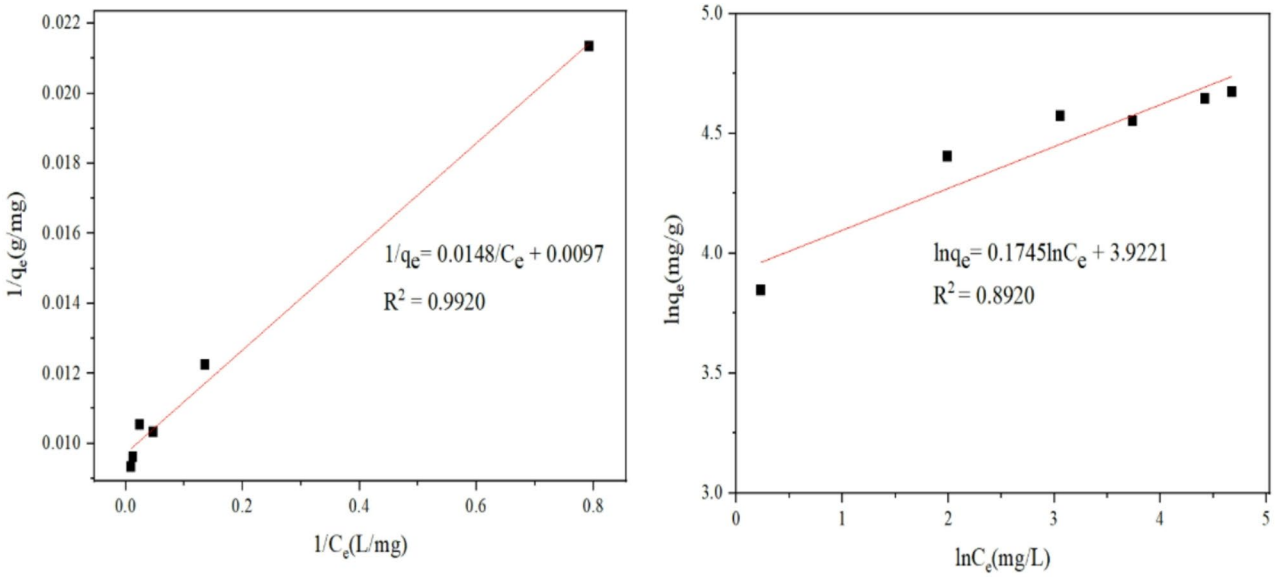

Fig. 5. Isotherm models for the adsorption of PO_4^{3-} on plane trees' bark biochar/ZnAl- LDH.

Temperature/℃	Langmuir			Freundlich		
	Q_{max} /(mg·g^{-1})	k_L/ (L·mg^{-1})	R^2	k_F /(mg$^{1-1/n}$·L$^{1/n}$·g^{-1})	$\frac{1}{n}$	R^2
25	103.1	0.6554	0.9920	22.48	0.1754	0.8920

Table 1. Adsorption isothermal parameters of PO_4^{3-} on plane trees' bark biochar/ZnAl-LDH (10 mg adsorbents, 25 mL of 20–150 mg/L PO_4^{3-}, 6 h, 25 °C).

based on the above analysis, 2 h was the adsorption equilibrium time. The temperature experiment shows that the high temperature is beneficial for the adsorption process (Fig. 4d). However, the adsorption ratio does not increase significantly, so the room temperature adsorption is more economical.

Adsorption isotherm study

The saturated adsorption capacity of PO_4^{3-} on plane trees' bark biochar/ZnAl-LDH was calculated by initial concentration adsorption data, which was fitted by both the classic Langmuir and Freundlich isotherm models. The adsorption data at 25 ℃ were linearly fitted in Fig. 5, and the relevant parameters were shown in Table 1. Moreover, the correlation coefficient (R^2) indicated that the adsorption process of Planed-Trees' bark/Zn-Al LDH for phosphate could be better explained by Langmuir equation, revealing the adsorption was mainly mono-molecular layer adsorption. As seen from Table 1, the saturated adsorption capacity was 103.1 mg/g, which indicates that the plane trees' bark biochar/ZnAl-LDH prepared by co-precipitation method has good adsorption capacity for phosphate ions in aqueous solution.

Adsorption kinetics study

According to the above two kinetic equations, the data of phosphate adsorption on the plane trees' bark biochar/ZnAl- LDH were fitted in Fig. 6, and the relevant parameters was shown in Table 2. From Table 2, it could be seen that R_2^2 was obviously better than R_1^2, and the adsorption capacity calculated by the quasi-second order kinetic equation approached to actual adsorption capacity, with a significant difference from that of the quasi-first order kinetic model. Therefore, the quasi-second order kinetic model could better describe the adsorption process of phosphate onto biochar/ZnAl-LDH, indicating that the adsorption of phosphate was mainly chemical adsorption.

Mechanism study of phosphate adsorption

As shown in Fig. 7, the new peaks appeared at 1038 cm^{-1} and 1365 cm^{-1} in the sample after adsorption, which belonged to the P-OH and P = O stretching vibration of phosphate. The above results proved that phosphate had been effectively adsorbed on the surface of the sample. Meanwhile, the infrared absorption peak at 1110 cm^{-1} conformed to stretching vibration peaks of SO_4^{2-}, and the intensity of infrared peak decreases after adsorption of phosphate, indicating that the sulfate between the layers was replaced by phosphate. Associated with XRD analysis, it could be concluded that the adsorbed phosphate was intercalated in the layers of the hydrotalcite, which was consistent with the structural characteristics of hydrotalcite-like materials[12]. In the range of 400 cm^{-1} to 700 cm^{-1}, the peaks of BC/ZnAl-LDH were characteristic lattice vibrations of M-OH (Zn-OH and Al-OH).

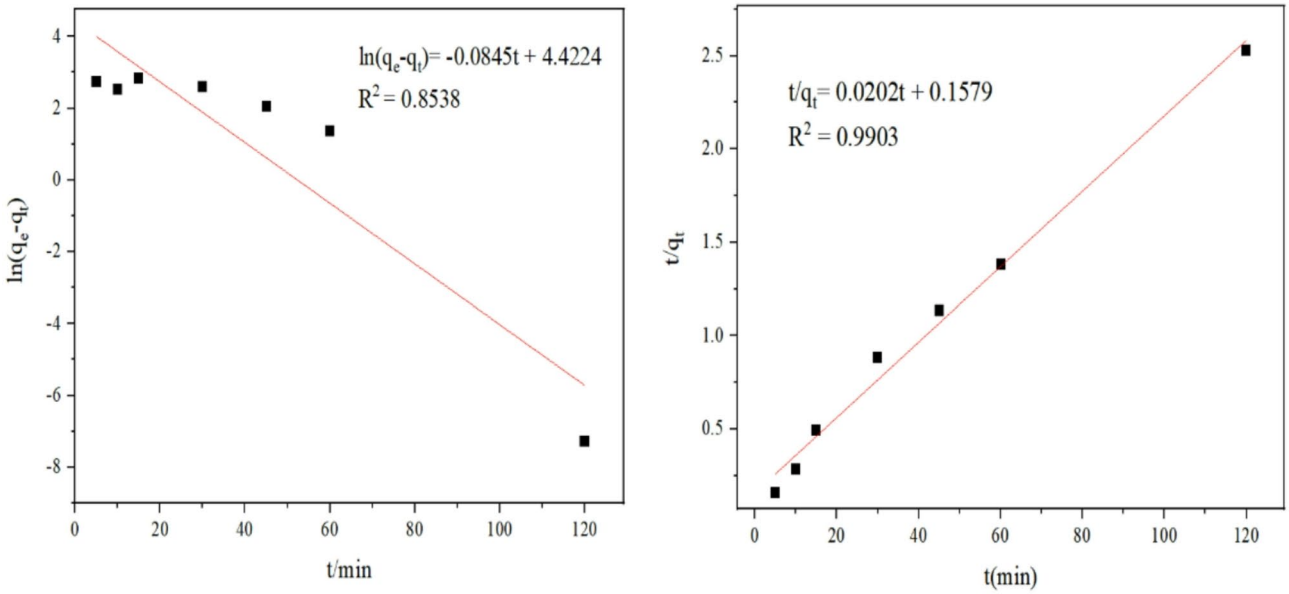

Fig. 6. Isotherm models for the adsorption of PO_4^{3-} on plane trees' bark biochar/ZnAl-LDH.

	Pseudo-first order kinetics				Pseudo-second order kinetics		
C_0/mg·g^{-1}	Q_e /mg·g^{-1}	$Q_{e,cal}$ /mg·g^{-1}	k_1 /10^{-2}min^{-1}	R_1^2	$Q_{e,cal}$ /mg·g^{-1}	k_2 /10^{-4}g·mg^{-1}·min^{-1}	R_2^2
20	46.5	0.3737	0.19	0.8538	49.5	2.6	0.9903

Table 2. Adsorption kinetic parameters of PO_4^{3-} on plane trees' bark biochar/ZnAl-LDH.

However, the intensity of these peaks decreased after P-adsorption, which indicated that M-OH was replaced by PO_4^{3-}. The new M-O-P composites was formed in the ways of Complexation or ligand exchange[10,11].

To find out the mechanism, XPS survey was also performed, and the results was shown in Fig. 8. There were the elements of C, O, Zn, and Al in the both biochar/ZnAl-LDH and biochar/ZnAl-LDH(P). Moreover, a notable P 2p peak appeared at 143.9 eV in the biochar/ZnAl-LDH(P), revealing the adsorbed phosphate onto biochar/ZnAl-LDH. The atomic ratio of the main elements such as C, O, Zn, Al in BC/ZnAl-LDH sample was 50.97%, 36.77%, 7.4% and 4.86%. After P adsorption, the atomic ratio of C, O, Zn, Al, P in BC/ZnAl-LDH(P) sample was 53.35%, 33.63%, 3.99% 3.22%, and 5.62%. Meanwhile, the S2p peak noticeably weakened because sulfate ions between layers were replaced by phosphate ions. The O1s spectrum of the biochar/ZnAl-LDH were composed of M-O (3.95%), M-OH (54.26%), C=O (12.31%), O-C=O (29.48%). However, after phosphate adsorption, the content of C=O and O-C=O decreased to 0.86% and 27.25% because part of CO_3^{2-} in the ZnAl-LDH was exchanged by PO_4^{3-}. The percentage of M-O increased fron 3.95–30.18%, while that of M-OH decreased from 54.26 to 41.69% due to replacement of OH by P-O bond. Similarly, in the both Zn2p and Al2p spectrum, the content of Zn-O and Al-O increased, and that of Zn-OH and Al-OH decreased. That may be due to the formation of P-O-Al and P-O-Mg bonds by ligand exchange or complexation. Above all, the adsorption mechanism of phosphate contained mainly interlayer anion exchange, surface complexion and ligand exchange[16,17].

Phosphorus recovery

10 mg of biochar/ZnAl-LDH composites were added to 7 mL of 50 mg/L PO_4^{3-} stirring for 2 h. Then, the sample of adsorbed phosphate were centrifuged to obtain the upper clear solution. The equilibrium concentration of phosphate (Ce) was determined by Phosphorus molybdenum blue spectrophotometric method. The phosphate removal ratio was 93% by 10 mg biochar/ZnAl-LDH for 7 mL of 50 mg/L PO43-. Then, the absorbed sample were soaked in 20% Na_2CO_3 solution for phosphate desorption, stirring for 2 h. The desorption efficiency (%) were calculated.

$$\text{Desorption efficiency } (\%) = \frac{\text{CPO}_4^{3-}(\text{Na}_2\text{CO}_3)}{\text{C}_0 - \text{C}_e} \times 100\%$$

After analysis, the desorption ratio was 61%, compared to the absorption ratio of 93%. The recovered phosphorus could be reused. In addition, the effect of Na_2CO_3 concentration on desorption efficiency were investigated. As shown in Fig. 9, it can be seen that in sodium carbonate solutions with mass ratios of 0.28%, 1.4%, 5.6%, 10%, and 20%, the desorption rates of phosphate ions are 13.8%, 26.1%, 57.4%, 56.3%, and 61.0%, respectively.

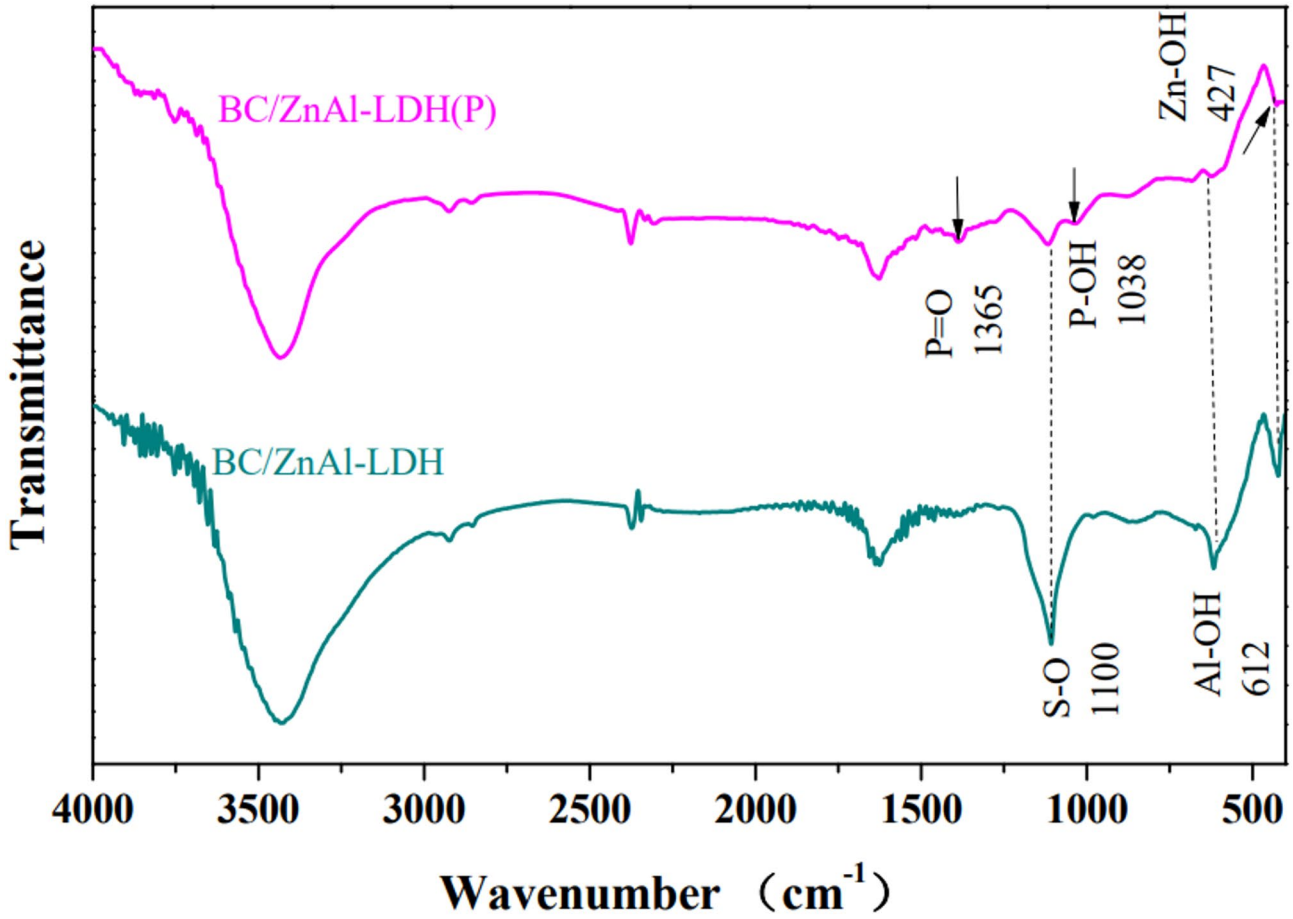

Fig. 7. FT-IR spectra of plane trees'bark biochar/ZnAl-LDH and plane trees'bark biochar/ZnAl-LDH (P).

Therefore, a suitable sodium carbonate desorption solution is around 5.5%. The desorption mechanism might be that adsorbed phosphate molecular could be replaced by the high concentration of CO_3^{2-} in the solution and phosphate molecular released[18].

The adsorption-desorption Cycle experiments have also been carried out in Fig. 10. The first round of adsorption was 93%, and that of desorption was 57.4%. The second round of adsorption was 38.64%, and that of desorption was 28.64%. This might be due to only a portion of the adsorbed phosphate in the first round were desorbed, and about 35.6% of the active sites still occupied. Therefore, the second round of adsorption was about 30%. The desorption ratio was 28.46%, and 73.65% of adsorbed PO_4^{3-} was released in the second round. Besides, the results revealed that single NaCl solution had no desorption effect for PO_4^{3-}. Since $Zn(OH)_2$ and $Al(OH)_3$ are amphoteric hydroxides, they are easily dissolved in both acidic and basic solutions. Above all, Na_2CO_3 solution was a suitable desorption solution. The phosphate adsorbed by ZnAl-LDH released, and it is expected to be reused.

Conclusion

The plane trees' bark biochar/ZnAl-LDH composites were prepared by the in-situ co-precipitation method. The adsorption isotherm of phosphate was mainly mono-molecular layer adsorption, with the saturated adsorption capacity of 101.3 mg/g. The adsorption process conformed to the second-order kinetics equation. Moreover, nearly 60% of the absorbed phosphate could be recovered in 5.5% Na_2CO_3 solution, and which may reuse in the future. The possible adsorption mechanism of phosphate mainly contained interlayer anion exchange, surface complexion and ligand exchange. Considering the sample was cheap and easy to prepare, it was expected to be applied in practical wastewater treatment containing phosphorus.

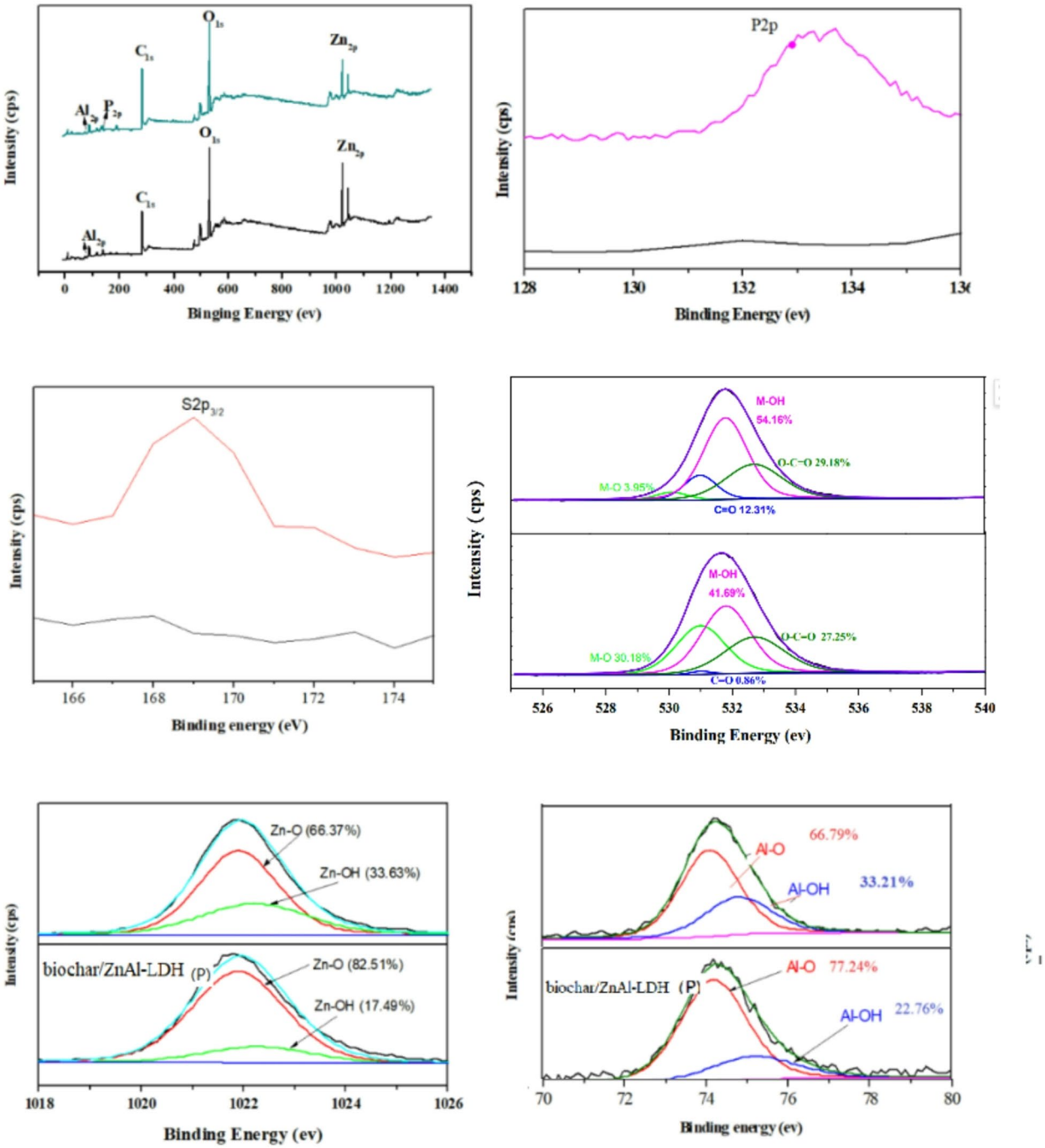

Fig. 8. XPS survey of biochar/ZnAl-LDH.

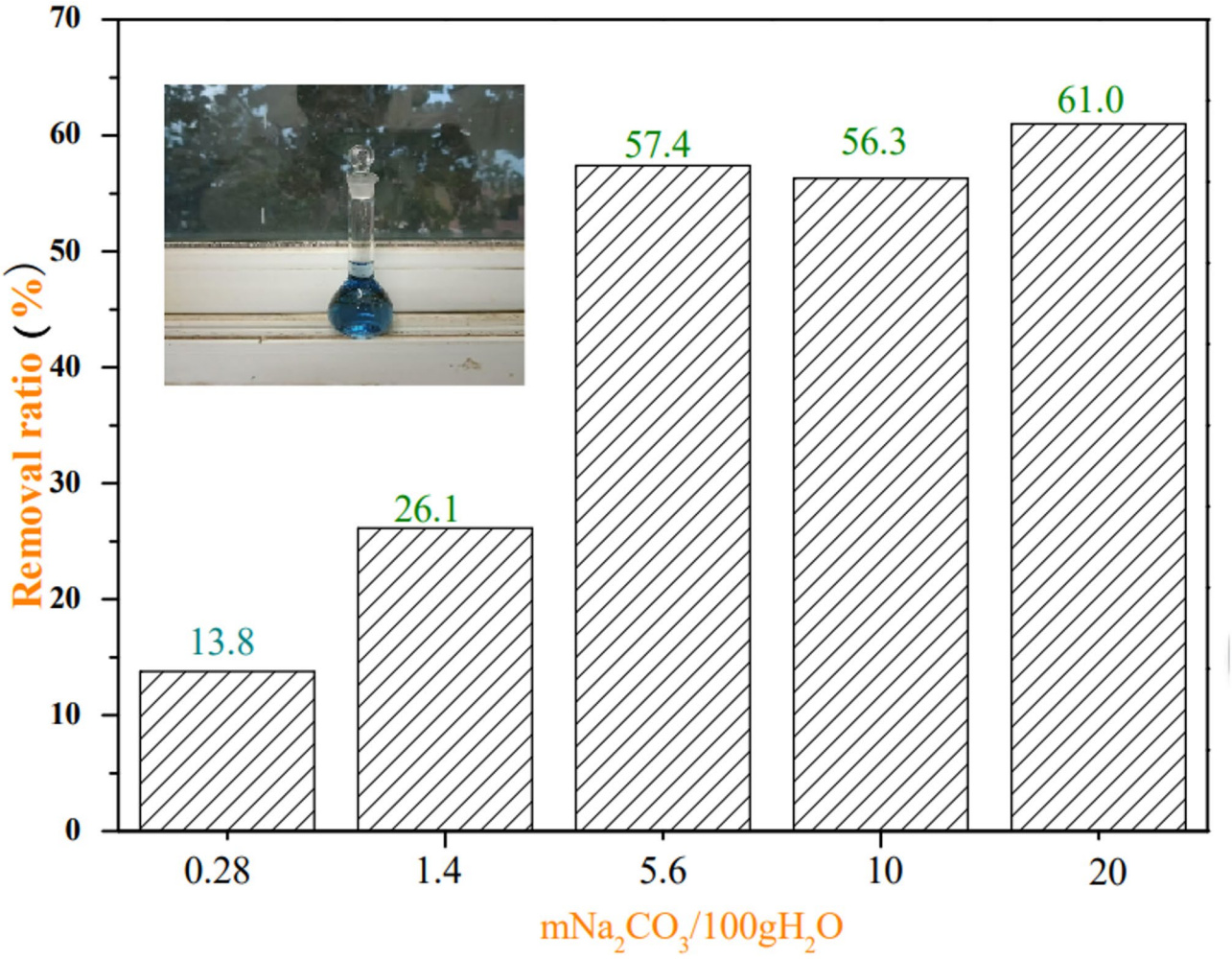

Fig. 9. the recovered phosphate in 10% Na_2CO_3 solution.

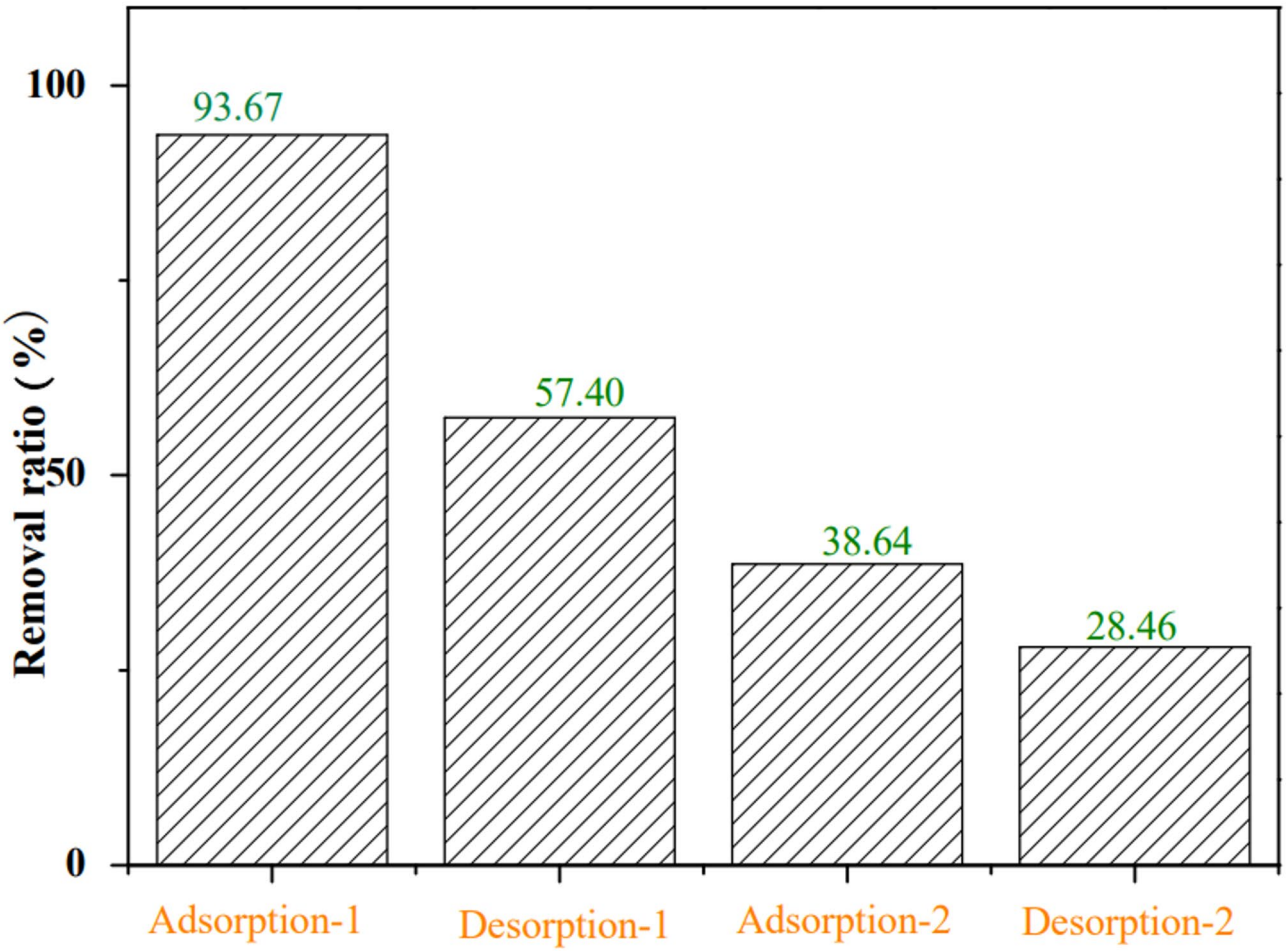

Fig. 10. The adsorption-desorption cycle experiment of phosphate onto biochar/ZnAl-LDH.

Data availability

Data is provided within the manuscript or supplementary information files.

Received: 18 December 2024; Accepted: 20 August 2025
Published online: 01 September 2025

References

1. Ye, Z. et al. Phosphorus recovery from synthetic swine wastewater by chemical precipitation using response surface methodology. *J. Hazard. Mater.* **176** (1–3), 1083–1088 (2010).
2. Guida, S. et al. Demonstration of ion exchange technology for phosphorus removal and recovery from municipal wastewater[J]. *Chem. Eng. J.* **420**, 129913 (2021).
3. Wang, Y. et al. Simultaneous removal of phosphorus and soluble organic pollutants by a novel organic/inorganic nanocomposite membrane via $Zr(OH)_4$ in-situ decoration. *J. Taiwan. Inst. Chem. Eng.* **131**, 104165 (2022).
4. Chen, Y. T. et al. Adsorption of PO_4^{3-}, Cd(II), Pb(II), Cu(II), As(III), and As(V) using a carbonised Mn-based metal–organic framework. *Arab. J. Chem.* **16**, 104950 (2023).
5. Kong, L. C. et al. Synchronous phosphate and fluoride removal from water by 3D rice-like lanthanum-doped la@mgal nanocomposites. *Chem. Eng. J.* **371**, 893 (2019).
6. Bernardo, M. P., Moreira, F. K. & Ribeiro, C. Synthesis and characterization of eco-friendly Ca-Al-LDH loaded with phosphate for agricultural applications. *Appl. Clay Sci.* **137**, 143–150 (2017).
7. Ogata, M. K. N. Properties of a novel adsorbent produced by calcination of nickel hydroxide and its capability for phosphate ion adsorption. *J. Ind. Eng. Chem.* **34**, 172–179 (2016).
8. He, H. et al. Efficient phosphate removal from wastewater by MgAl-LDHs modiffed hydrochar derived from tobacco stalk. *Bioresour Technol. Rep.* **8**, 100348 (2019).
9. Rahman, S. et al. High capacity aqueous phosphate reclamation using Fe/Mg-layered double hydroxide (LDH) dispersed on Biochar. *J. Colloid Interface Sci.* **597**, 182–195 (2021).
10. Peng, Y. et al. Optimizing the synthesis of fe/al (Hydr) oxides-Biochars to maximize phosphate removal via response surface model. *J. Clean. Prod.* **237**, 117770 (2019).
11. Peng, G. et al. Synthesis of mn/al double oxygen Biochar from dewatered sludge for enhancing phosphate removal. *J. Clean. Prod.* **251**, 119725 (2020).
12. Seftel, E. M. et al. Insights into phosphate adsorption behavior on structurally modified ZnAl layered double hydroxides. *Appl. Clay Sci.* **165**, 234–246 (2018).

13. Kim, T. H., Lundehj, L. & Nielsen, U. G. An investigation of the phosphate removal mechanism by MgFe layered double hydroxides. *Appl. Clay Sci.* **189**, 105521 (2020).
14. Liu, Q., Zhang, L. H. & Zhou, Y. B. Zn–Al hydrotalcites and magnetic Zn–Al hydrotalcites for efficient phosphate remediation and recovery. *Russ J. Phys. Chem. A*. **97** (14), 3388–3398 (2024).
15. Yao, Y., Gao, B., Chen, J. & Yang, L. Engineered Biochar reclaiming phosphate from aqueous solutions: mechanisms and potential application as a slow-release fertilizer. *Environ. Sci. Technol.* **47**, 8700–8708 (2013).
16. Cuong, D. V. & Hou, C. H. Enhancing phosphorus removal through layered double hydroxide-decorated biochars: unveiling pore structure and surface functionalization. *J. Taiwan. Inst. Chem. E.* **155**, 105273 (2024).
17. Wu, Y. et al. Effective removal of pyrophosphate by Ca–Fe–LDH and its mechanism. *Chem. Eng. J.* **179**, 72 (2012).
18. Luo, D. et al. Phosphorus adsorption by functionalized biochar: a review. *Environ. Chem. Lett.* **21**, 1–28 (2022).

Acknowledgements

This work was financially supported by Doctor Foundation of Pingdingshan University (PXYBSQD-2015004), the Key scientific research projects in Henan Province's University (25B150028), and the National Natural Science Foundation of China (Grant Nos.21605090). We thank the Analytical Center of Pingdingshan University and Changchun Institute of Applied Chemistry for characterizing the samples.

Author contributions

Lihui Zhang* and Caoyang Zhang, conducted the experimental data supplementation in the revised manuscript, analyzed data and wrote the paperChen Zhang, conducted primary experimentsWeili Li, Yanbiao Zhou， Yabo Wang, Gangfeng Du Checked the paper.

Declarations

Competing interests

The authors declare no competing interests.

Additional information

Correspondence and requests for materials should be addressed to L.Z.

Reprints and permissions information is available at www.nature.com/reprints.

Publisher's note Springer Nature remains neutral with regard to jurisdictional claims in published maps and institutional affiliations.